Available online at www.sciencedirect.com
SCIENCE DIRECT®
PHYSICS LETTERS A
ELSEVIER
Physics Letters A 314 (2003) 140–149
www.elsevier.com/locate/pla

# On periodic inertia–gravity waves of finite amplitude propagating without change of form at sharp density-gradient interfaces in the rotating fluid

R. Plougonven, V. Zeitlin *

*Laboratoire de Meteorologie Dynamique, Ecole Normals Superieure, 24 rue Lhomond, 75231 Paris Cedex 05, France*

Received 31 January 2003; received in revised form 19 May 2003; accepted 23 May 2003

Communicated by A.P. Fordy

**Abstract**

Existence of finite-amplitude inertia–gravity waves propagating without change of form is proved in the two-layer rotating shallow water model. We find exact solutions of the full equations of motion corresponding to such waves. The form of the nonlinear waves depends on the parameters of the model (density and height ratios of the layers) and on the phase speed. Three distinct families of waves having different forms and responding differently to the increase of amplitude are identified.


## 1. Introduction

The inviscid hydrostatic rotating shallow-water model (RSW) is widely used in geophysical fluid dynamics (GFD), cf., e.g., [1]. In the pioneering papers [5,6] V. Shrira has found specific exact solutions in this model in the form of finite-amplitude periodic plane-parallel waves (see also a recent review [2]). This fact is rather surprising if one recalls that RSW is a hyperbolic system of gas-dynamics type and exhibits wave-breaking and shock formation (cf. [3,7]). In the limit of small amplitudes the nonlinear waves tend to the well-known infinitesimal surface inertia–gravity waves. The amplitude of the fully nonlinear waves is limited from above and the waves tend to form cusps at their crests while approaching the limiting amplitude. Thus, although weak, the dispersion introduced by rotation at the long-wave end of the spectrum is sufficient to counter-balance the nonlinearity and to lead to the formation of stationary waves in the periodic geometry (there are no solitary waves in the model).

Besides rotation, the second fundamental phenomena in GFD is stratification. It is absent in the barotropic one-layer RSW model but may be introduced, in the simplest way, by superimposing several RSW layers of different densities. Such multi-layer models are of frequent use in GFD [1,4] (e.g., in the oceanic thermocline context), in particular the two-layer one. In order to pinpoint the purely baroclinic phenomena the rigid lid upper boundary condition may be used, thus

* Corresponding author.
*E-mail address:* zeitlin@lmd.ens.fr (V. Zeitlin).

0375-9601/03/$ – see front matter 
doi:10.1016/S0375-9601(03)00882-X

reducing dynamics to the interface between the two layers. Below we show that nonlinear periodic waves also exist in the two-layer RSW but depending on the parameters of the model and on the phase velocity, their form varies falling into three distinct families.

## 2. Stationary waves of finite amplitude in the one-layer RSW

We first remind the derivation of the nonlinear wave solutions in the one-layer case. The same standard method will be used afterward in the two-layer case. The equations of the RSW model reduced to the plane-parallel solutions (i.e., those independent on one spatial coordinate, $y$) consist of the horizontal momentum conservation equations in the presence of the Coriolis force and the hydrostatic pressure force (the centrifugal force, as usual in the GFD applications, is neglected) and the mass conservation equation:

$$\partial_t u + u\partial_x u - fv + g\partial_x h = 0, \tag{1a}$$

$$\partial_t v + u\partial_x v + fu = 0, \tag{1b}$$

$$\partial_t h + \partial_x (uh) = 0. \tag{1c}$$

Here $f$ is the Coriolis parameter (the double of the angular velocity of rotation), $g$ is the acceleration due to gravity, $u, v$ are the two components of the horizontal fluid velocity, $h$ is the free surface elevation. We look for stationary propagating solutions depending on $\xi = x - ct$ only; the prime will denote the derivative with respect to $\xi$. Therefore,

$$-cu' + uu' - fv + gh' = 0, \tag{2a}$$

$$-cv' + u(f + v') = 0, \tag{2b}$$

$$-ch' + (uh)' = 0. \tag{2c}$$

Integration of (2c) gives $u = c + K/h$, where $K$ is an integration constant. As we look for spatially periodic solutions with a (yet unknown) wavelength $\lambda$ and with no overall mass-flux in the $x$ direction, integrating $uh$ over one wavelength $\lambda$ gives zero:

$$\int_0^\lambda (K + ch)\, d\xi = 0. \tag{3}$$

Hence, the value of the integration constant is $K = -cH$, where $H$ is the mean elevation (or the rest height) of the fluid, yielding for $u$:

$$u = c\left(1 - \frac{H}{h}\right). \tag{4}$$

Note that solutions we are looking for bear no potential vorticity anomaly, just as linear inertia–gravity waves. Indeed, potential vorticity (PV) which is a material invariant of the system (1) defined as

$$q = \frac{f + \partial_x v}{h} \tag{5}$$

by virtue of (2b) and (4) is equal to

$$q = \frac{f + v'}{h} = \frac{f}{H}, \tag{6}$$

i.e., the background PV of the unperturbed fluid layer.

We introduce the dimensionless elevation $\chi$: $h = H\chi$, define the Mach (or Froude) number $M = c/\sqrt{gH}$ and from (4) and (2), obtain the following equation for $\chi$:

$$\left[\frac{M^2}{2}\frac{1}{\chi^2} + \chi\right]'' - \frac{f^2}{c_0^2}(\chi - 1) = 0. \tag{7}$$

From this equation we get

$$1 - \frac{M^2}{\chi^3} = \frac{f^2}{c_0^2}\frac{\chi - 1}{\chi''}. \tag{8}$$

At the wave-crest we have $\chi - 1 > 0$, $\chi'' < 0$, and hence the r.h.s. of the expression above is negative. Therefore, $1 < \chi^3 < M^2$ and necessarily $M > 1$.

After multiplication by $\left[\frac{M^2}{2}\frac{1}{\chi^2} + \chi\right]'$ Eq. (7) may be integrated once, and reduced to a "particle-in-a-well" equation at zero energy level of the "particle":

$$\chi'^2 + \frac{f^2}{c_0^2}\mathcal{V}(\chi; M, \mathcal{A}) = 0. \tag{9}$$

Note that only strictly positive values of $\chi$ are physically meaningful. The expression for the potential energy is:

$$\mathcal{V}(x; M, \mathcal{A}) = \frac{\mathcal{N}(\chi; M, \mathcal{A})}{(\mathcal{D}(\chi; M, \mathcal{A}))^2} = \frac{(\chi - 1)^2\left(\frac{M^2}{\chi^2} - 1\right) - \mathcal{A}}{\left(\frac{M^2}{\chi^3} - 1\right)^2}. \tag{10}$$

Here $\mathcal{A}$ is an integration constant. Inserting, e.g., the value $\chi = 1$, it can be easily seen that $\mathcal{A}$ is necessarily non-negative (it is zero for the fluid at rest, strictly positive otherwise, and increases with the amplitude of the wave solutions to be obtained).

Stationary waves of finite amplitude correspond to the oscillations of the particle around the rest position $\chi = 1$. They exist if the potential has a zone of values which are negative and bounded from below, and if this zone is situated between two strictly positive zeros,[1] $\chi_l$ and $\chi_r$, with 1 in between: $0 < \chi_l < 1 < \chi_r$. Such zone will be called a well below. An elementary analysis shows that: the denominator $(\mathcal{D})^2$ is always positive; thus the sign of the potential is determined by the numerator; $\mathcal{D}$ has a unique zero for $\chi_0 = M^{2/3} > 1$ (cf. the gray curve in Fig. 1(a), (b), (c)). The numerator $\mathcal{N}$ tends to $+\infty$ as $\chi \to 0$; for $\chi = 1$, it is equal to $-\mathcal{A}$ and, hence, is strictly negative for positive $\mathcal{A}$. Therefore, there is a zero of $\mathcal{N}$ in the interval $]0, 1[$.

For $\chi \to +\infty$, $\mathcal{N} \to \infty$, and $\mathcal{N}$ has a single maximum in $]1, +\infty[$. This maximum occurs for the same value of $\chi$ as the zero of the denominator: $\chi_0 = M^{2/3} > 1$. Therefore, if $\mathcal{N}(\chi_0; M, \mathcal{A})$ is strictly positive, the numerator has one zero in the interval $]1, \chi_0[$: the potential then has a well and stationary waves exist. For $\mathcal{A}$ close to zero, it is easy to check that the numerator has two zeros close to 1, and waves of small amplitude always exist. For small deviations from the rest-state, (9) becomes the harmonic oscillator equation with (spatial) frequency

$$k^2 = \frac{1}{M^2 - 1}. \tag{11}$$

This expression is equivalent to the well-known dispersion relation for linear surface inertia–gravity waves $c^2 = gH(1 + k^{-2})$. As $\mathcal{A}$ increases, the graph of $\mathcal{N}$ is translated downward (cf. the dashed curve in Fig. 1(a), (b), (c)) and there exists a critical value $\mathcal{A}_c$ for which the maximum of the numerator in $]1, +\infty[$ is zero: $\mathcal{N}(\chi_0; M, \mathcal{A}) = 0$. Asymptotic analysis in the vicinity of $\chi_0 = M^{2/3}$ then shows that the potential itself is continuous and has no well: hence, waves exist only for $0 < \mathcal{A} < \mathcal{A}_c$. Note that as $\mathcal{A}$ increases, the potential becomes more and more asymmetric. Correspondingly, the wave-crests sharpen, and the waves tend to develop cusps as $A \to A_c$ (cf. Fig. 1). However, as it was shown in [7] a true cusp is an asymptotic envelope of the solutions and is not attainable.

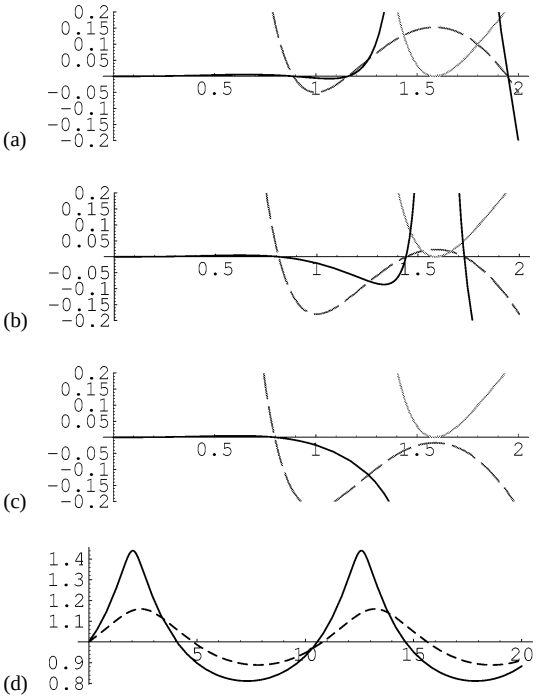


Fig. 1. (a), (b), and (c): The numerator $\mathcal{N}$ (dashed), the denominator $(\mathcal{D})^2$ (gray, dotted) of the potential $\mathcal{V}$ and the potential itself (plain) for $M = 2$ and increasing values of $\mathcal{A}$: (a) $\mathcal{A} = 0.05$, (b) $\mathcal{A} = 0.18$, and (c) $\mathcal{A} = 0.22$. In the last case, the numerator has no zero in $]1, +\infty[$, hence the potential has no well and there are no stationary waves, (d) wave profiles for $\mathcal{A} = 0.05$ (dashed) and $A = 0.18$ (plain).

Summarizing, stationary waves exist if the equation

$$\mathcal{N}(\chi; M, \mathcal{A}) = (\chi - 1)^2\left(\frac{M^2}{\chi^2} - 1\right) - \mathcal{A} = 0 \tag{12}$$

has two distinct roots in the interval $]1, +\infty[$ or, equivalently, if $\mathcal{N}(M^{2/3}; M, \mathcal{A}) > 0$. The height of the crests of the waves is bounded from above by the limiting value $M^{2/3}$. The difference between the roots of the numerator gives the amplitude of the wave; its wavelength depends on the value of the parameter $f^2/c_0^2$.

The obtained nonlinear waves are thus the plane-parallel surface inertia–gravity waves of finite amplitude. Note that they are not strictly one-dimensional as

[1] A zero value of $h$ is unacceptable as it leads to infinite $u$, cf. (4).

the cross-propagation velocity $v$ is nonzero and varies periodically (cf. Eq. (2b)).

## 3. Stationary waves of finite amplitude in the 2-layer model

We show below that the two-layer RSW model also admits propagating waves of finite amplitude as exact periodic solutions of the equations of motion. In some regimes of parameters they are analogous to those found in the one-layer model. However, other regimes exhibiting different behavior specific to the two-layer model exist. Three different families of waves will be identified below.

Following the same standard approach as in the one-layer case, a governing equation for stationary waves will be derived. The waves will be again identified with the oscillations of a particle in a well; the corresponding potential will be studied and the bifurcations between the wave-families in the parameter space will be described.

### 3.1. General equation for the stationary waves

The equations of the two-layer rotating shallow water model with no variations in the $y$ direction are:

$$\partial_t u_1 + u_1\partial_x u_1 - f v_1 + \rho_1^{-1}\partial_x \pi = 0, \tag{13a}$$

$$\partial_t v_1 + u_1(f + \partial_x v_1) = 0, \tag{13b}$$

$$\partial_t u_2 + u_2\partial_x u_2 - f v_2 + \rho_2^{-1}\partial_x \pi + g'\partial_x h = 0, \tag{13c}$$

$$\partial_t v_2 + u_2(f + \partial_x v_2) = 0, \tag{13d}$$

$$\partial_t (H - h) + \partial_x((H - h)u_1) = 0, \tag{13e}$$

$$\partial_t h + \partial_x (h u_2) = 0 \tag{13f}$$

where $u_i, v_i$, $i = 1, 2$, are the velocities in the upper and the lower layer, respectively; $\pi$ is the barotropic pressure imposed by the rigid lid; $h(x, t)$ is the elevation of the interface between the layers, $H_1$ and $H_2$ are the heights of the two layers at rest ($H = H_1 + H_2$ is the total height and $h$ may vary within the limits $[0, H]$); $g'$ is the so-called reduced gravity: $g' = g(\rho_2 - \rho_1)/\rho_2$.

We look for stationary wave solutions which are functions of $\xi = x - ct$ and obtain the following system of ODEs (the prime denotes the $\xi$-derivative, as usual):

$$-cu_1' + u_1 u_1' - f v_1 + \rho_1^{-1}\pi' = 0, \tag{14a}$$

$$-cv_1' + u_1(f + v_1') = 0, \tag{14b}$$

$$-cu_2' + u_2 u_2' - f v_2 + \rho_2^{-1}\pi' + g' h' = 0, \tag{14c}$$

$$-cv_2' + u_2(f + v_2') = 0, \tag{14d}$$

$$-c(H - h)' + (u_1(H - h))' = 0, \tag{14e}$$

$$-ch' + (u_2 h)' = 0. \tag{14f}$$

The last two equations can be directly integrated:

$$u_1 = c + \frac{C_1}{H - h}, \qquad u_2 = c + \frac{C_2}{h}, \tag{15}$$

where $C_1$ and $C_2$ are the integration constants. The zero-flux condition $u_1(H - h) + u_2 h = 0$ yields:

$$C_1 + C_2 = -cH. \tag{16}$$

The expressions (15) are then inserted into (14a) and (14c), $v_1'$ and $v_2'$ are eliminated using (14b) and (14d) and the following single equation for $h$ follows:

$$\left[\frac{1}{2}\left(\frac{C_2}{h}\right)^2 - \frac{r}{2}\left(\frac{C_1}{H - h}\right)^2 + g' h\right]'$$
$$+ cf^2\left(\frac{1}{C_2} + \frac{r}{C_1}\right)h$$
$$+ f^2\left(1 - r - r\frac{cH}{C_1}\right) = 0, \tag{17}$$

where $r = \rho_1/\rho_2$ is the ratio of the densities of the layers. We are looking for periodic solutions with a certain period $\lambda$. By integrating (17) over one period and using the fact that the integral of the interface position $h$ over the period is $H_2$ by definition, we get the following constraint:

$$1 + \frac{cH_2}{C_2} - r\left(1 + \frac{cH_1}{C_1}\right) = 0, \tag{18}$$

which, together with (16), allows to fix the values of $C_1$ and $C_2$: $C_1 = -cH_1$, $C_2 = -cH_2$, and to determine $u_1$ and $u_2$:

$$u_1 = c\frac{-(h - H_2)}{H - h}, \qquad u_2 = c\frac{h - H_2}{h}. \tag{19}$$

Eq. (17) then becomes:

$$\left[\frac{c^2}{2}\left(\left(\frac{H_2}{h}\right)^2 - r\left(\frac{H_1}{H - h}\right)^2\right) + g' h\right]'$$
$$- \frac{f^2}{H_e}(h - H_2) = 0, \tag{20}$$

where we introduced the equivalent depth $H_e = \frac{H_1 H_2}{H_1 + r H_2}$. As in the one-layer case, the PV-anomaly in each layer is zero, as may be easily seen by using (14b), (14d), and (19). We thus get

$$q_1 = \frac{f}{H_1}, \qquad q_2 = \frac{f}{H_2}. \tag{21}$$

Introducing the nondimensional variable $\chi = h/H$, and the notation

$$\gamma = \frac{H_2}{H}, \qquad M = \frac{c}{\sqrt{g' H_e}} = \frac{c}{c_e},$$
$$\varphi(r,\gamma) = \frac{H_e}{H} = \frac{(1-\gamma)\gamma}{(r\gamma + 1 - \gamma)}$$

we rewrite (20) as:

$$\left[\frac{M^2\varphi(r,\gamma)}{2}\left(\frac{\gamma^2}{\chi^2} - r\frac{(1-\gamma)^2}{(1-\chi)^2}\right) + \chi\right]'' - \frac{f^2}{c_e^2}(\chi - \gamma) = 0. \tag{22}$$

This equation is similar to (7), but the first term here diverges both at $\chi \to 0$ and $\chi \to 1$, i.e., when the interface approaches either of the horizontal boundaries. It is easy to check that in the limit $H_1 \to \infty$, Eq. (20) takes the form of the equation for nonlinear waves in the one-layer model with the replacements $H \to H_2$, $g \to g'$. It can also be seen that the linearization of (20) for $\chi$ close to $\gamma$, $\eta = \chi - \gamma \to 0$ gives

$$\left(g' H_e - c^2\right)\eta'' - f^2\eta = 0, \tag{23}$$

with the dispersion relation for linear internal inertia-gravity waves which follows: $c^2 = g' H_e(1 + k^{-2})$.

After multiplication by the first derivative of the expression in the square brackets, (22) may be integrated once and gives:

$$\chi'^2 + \frac{f^2}{c_e^2}\mathcal{V}_2(\chi; M, r, \gamma, \mathcal{A}) = 0, \tag{24}$$

where

$$\mathcal{V}_2(\chi; M, r, \gamma, \mathcal{A}) = \frac{\mathcal{N}_2}{(\mathcal{D}_2)^2} = \frac{(\chi-\gamma)^2\left[\varphi M^2\left(\frac{\gamma}{\chi^2} + r\frac{1-\gamma}{(1-\chi)^2}\right) - 1\right] - \mathcal{A}}{\left(\varphi M^2\left(\frac{\gamma^2}{\chi^3} + r\frac{(1-\gamma)^3}{(1-\chi)^3}\right) - 1\right)^2}, \tag{25}$$

is the potential, playing the same role as $\mathcal{V}$ in the one-layer case. Only values of $\chi$ between 0 and 1 are physically meaningful. As in the one-layer case $\mathcal{A} > 0$ and $M > 1$.

### 3.2. Analysis of the potential $\mathcal{V}_2$

The structure of the potential is similar to that of the potential $\mathcal{V}$ in the one-layer case. However, there are two additional parameters, the ratios of the heights and densities of the two layers, respectively $\gamma$ and $r$, and the numerator and denominator now diverge at two points: $\chi \to 0$ and $\chi \to 1$. In order to have stationary waves, a well in the potential is needed around the rest state $\chi = \gamma$. The structure of the potential is as follows:

The denominator $(\mathcal{D}_2)^2$ is always positive; the sign of the potential is given by the sign of the numerator. The numerator $\mathcal{N}_2$ tends to $+\infty$ for $\chi \to 0$ and for $\chi \to 1$. Furthermore, for $\chi \to \gamma$

$$N_2(\chi, M, \mathcal{A}, r, \gamma) \sim (\chi - \gamma)^2\left(M^2 - 1\right) - \mathcal{A}, \tag{26}$$

with $\mathcal{A} > 0$. Hence, $\mathcal{N}_2$ has at least one zero in each interval $]0, \gamma[$ and $]\gamma, 1[$. Only the zeros closest to $\gamma$, $\chi_l$ and $\chi_r$, respectively, matter. The possibility of having waves in the system depends on the behavior of the denominator: in order to have wave solutions it is sufficient that the denominator does not have zeros in the interval $[\chi_l, \chi_r]$. Note that the derivative of $\mathcal{N}_2$ with respect to $\chi$ is equal to $2(\chi - \gamma)\mathcal{D}_2$. Therefore, once again, local extrema of the numerator other than $\chi = \gamma$ coincide with the zeros of $\mathcal{D}_2$.

The square root of the denominator, $\mathcal{D}_2$ tends to $+\infty$ at $\chi \to 0$ and $\chi \to 1$, and has a single minimum in between. Elementary analysis shows that the minimum corresponds to

$$\chi_m(r,\gamma) = -\frac{1}{1 + r^{1/4}\left(\frac{1-\gamma}{\gamma}\right)^{1/2}}. \tag{27}$$

Note that the location of this minimum is a function of parameters $r$ and $\gamma$ only. If $\mathcal{D}_2(\chi_m; M, r, \gamma) > 0$, the denominator never vanishes in $]0, 1[$, and hence wave solutions always exist, whatever the value of $\mathcal{A}$. If $\mathcal{D}_2(\chi_m; M, r, \gamma) = 0$, the denominator vanishes only at the point $\chi_m$, while if $\mathcal{D}_2(\chi_m; M, r, \gamma) < 0$ it has two zeros, one on each side of $\chi_m$. It is then necessary to investigate the location of the numerator's roots relative to the denominator's ones.

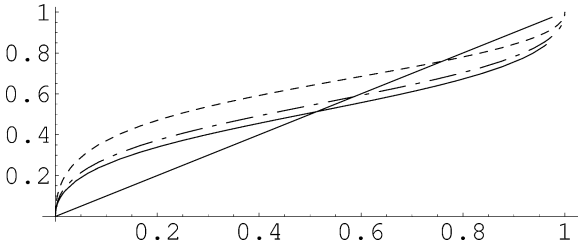


Fig. 2. Minimum of $\mathcal{D}_2$, i.e., $\chi_m(r,\gamma)$, as a function of $\gamma$, for various values of $r$: 0.9 (plain), 0.5 (dot-dashed), 0.1 (dashed). $\gamma$ is also plotted (straight line) in order to determine solutions to $\chi_m(r,\gamma_0)=\gamma_0$. The solution to this equation tends to 0.5 at $r\to 1$, and to 1 at $r\to 0$.

The existence (or nonexistence) of wave solutions follows from the existence (or nonexistence) of zeros in the denominator. The following observation on the position of zeros of the denominator with respect to the rest position $\chi=\gamma$ is crucial. For $\chi=\gamma$ the denominator is equal to $(M^2-1)^2>0$. Two properties of the denominator then follow:

- For any given value of $r$, there always exists a value of $\gamma$ such that the denominator never vanishes: this value $\gamma_0(r)$ is given by $\chi_m(r,\gamma_0)=\gamma_0$. In this case stationary wave solutions exist for any $\mathcal{A}$. For example, for layers of close densities (the plain curve in Fig. 2), waves exist for any $\mathcal{A}$ at least for a value of $\gamma$ close to 0.5.
- If $\mathcal{D}_2$ has two zeros, both are situated either in the interval $]0,\gamma[$ or in the interval $]\gamma,1[$.[2] The location of zeros of $\mathcal{D}_2$ determines the orientation of the cusp-like features. For $\gamma$ greater than $\gamma_0(r)$ (or equivalently $\chi_m(r,\gamma)<\gamma$), cusps are downward-oriented, for $\gamma$ below $\gamma_0(r)$, cusps are upward-oriented. For example, as seen from Fig. 2, if cusps form in the case $\gamma<0.5$, they are oriented upward.

### 3.3. Wave families

As a result we have three families of waves.

**Family A**. $\mathcal{D}_2(\chi_m(r,\gamma);M,r,\gamma)\leqslant 0$ and $\gamma<\gamma_0(r)$.

[2] More precisely, if $\gamma<\gamma_0(r)$, both are in $]\gamma,1[$, and if $\gamma>\gamma_0(r)$, both are in $]0,\gamma[$.

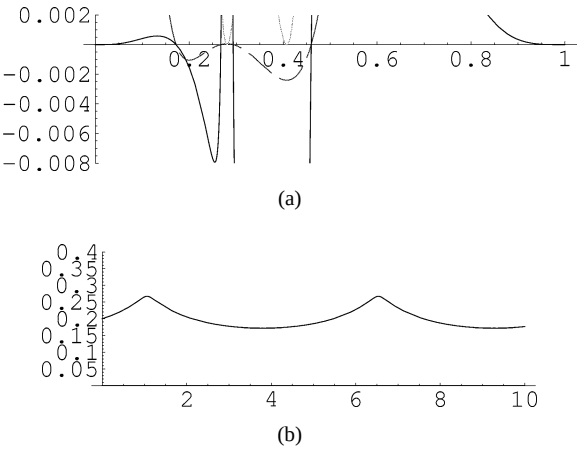


Fig. 3. Typical potential and wave profile for family A: (a) $\mathcal{N}_2$ (dashed), $\mathcal{D}_2$ (gray, dotted), and potential $\mathcal{V}_2$ for $M=1.35$, $r=0.9$, $\gamma=0.2$ and $\mathcal{A}=0.00105$. $\mathcal{A}$ is chosen near the critical value. The denominator has two zeros; as can be seen, they are also zeros of the derivative of the numerator, (b) profile of the corresponding wave (plain).

The corresponding waves behave qualitatively in the same manner as waves of the one-layer RSW: there exists a limiting amplitude, the wave profiles tend to develop cusps at their crests as the amplitude approaches the critical one. An example of the potential and of the corresponding wave profile is shown in Fig. 3. The response of the waves of this family to the increase of amplitude is shown in Fig. 4. The cusp is an asymptotic limit and, in fact, no discontinuity is realized, for the same reasons as in the one-layer case (cf. [7]).

Qualitatively, waves of the family A arise when the depth of the upper level is considerably larger than the depth of the lower layer (what "considerably" precisely means depends on the values of other parameters).

**Family B**. $\mathcal{D}_2(\chi_m(r,\gamma);M,r,\gamma)>0$.

In the absence of zeros in the denominator, the potential always has a well around $\chi=\gamma$, whatever the value of $\mathcal{A}$. Hence, formally, there is no limiting amplitude for the waves other than that imposed by the boundaries. Profiles of the waves of this family for given values of $M$ and $r$, and for various amplitudes are shown in Fig. 5.

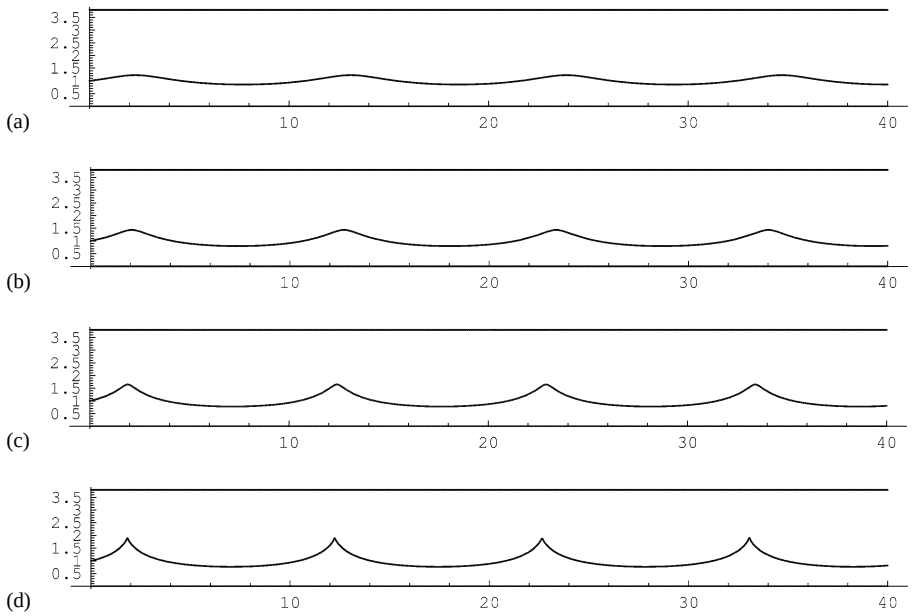


Fig. 4. Response of the waves of the family A to the increase of amplitude (from top to bottom). Panel (d) shows a wave approaching the limiting amplitude. Parameter values are $H_1 = 1$, $H_2 = 2.8$, $r = 0.1$ and $M = 2$.

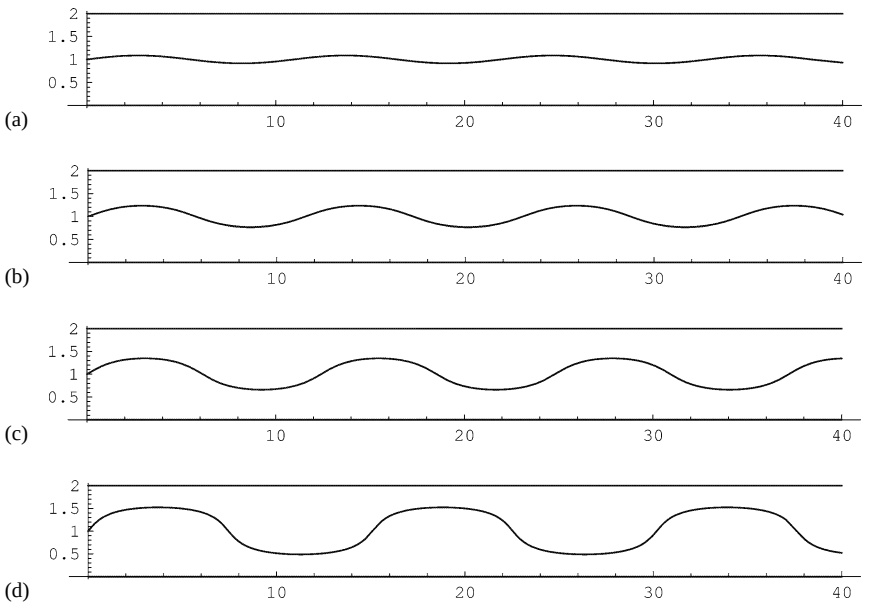


Fig. 5. Waves of the family B: these waves 'feel' the presence of the rigid lid and are bounded only by the lower and upper boundaries. Parameters are: $H_1 = 1$, $H_2 = 1$, $r = 0.9$ and $M = 2$.

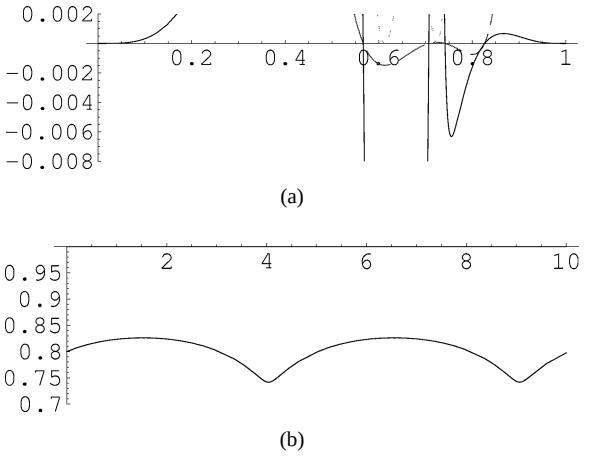


Fig. 6. Potential and wave profile for a wave of family C, represented in the same way as in Fig. 3. The values of the parameters are $M = 1.3$, $r = 0.9$, $\gamma = 0.8$ and $\mathcal{A} = 0.00075$. As $\mathcal{A}$ approaches the limiting value, the profile tends to develop cusps at the troughs.

**Family C**. $\mathcal{D}_2(\chi_m(r,\gamma); M, r, \gamma) \leqslant 0$ and $\gamma > \gamma_0(r)$.

Qualitatively, these waves are the upside-down version of the waves of the family A, as shown in Fig. 6. They are limited by a critical amplitude and tend to form cusps at the troughs as their amplitude increases. They correspond to the situation when the depth of the lower layer is considerably larger than the depth of the upper one.

### *3.4. Bifurcations in the parameter space*

For a given value of $r$, the domains corresponding to the families A, B, and C in the parameter space $(M, \gamma)$ may be obtained by plotting the curve corresponding to the zero level of $\mathcal{D}_2(\chi_m; M, r, \gamma)$ as shown in Fig. 7. Crossing this curve corresponds to a bifurcation. For instance, for given values of $\gamma$ and $r$, one can switch from the family A to the family B

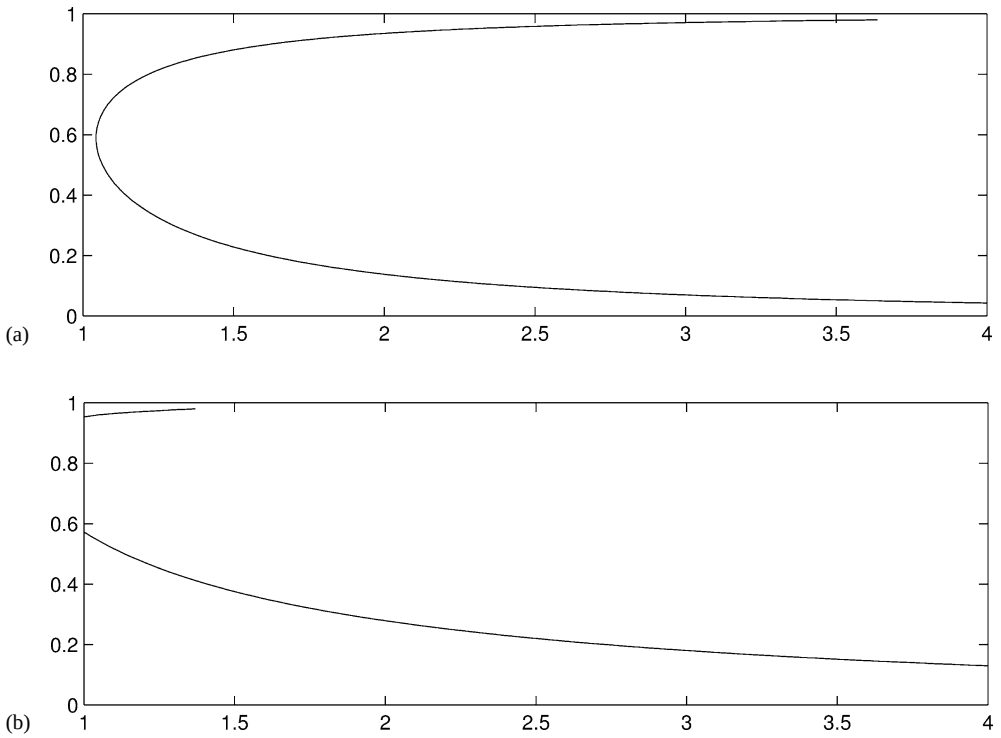


Fig. 7. Separation in $(M, \gamma)$ space between parameter regimes corresponding to the waves of family A (bottom region), B (center) and C (top region), for (a) $r = 0.9$ and (b) $r = 0.1$. As the difference between the densities of the two layers increases, the domain in parameter space corresponding to family C shrinks.

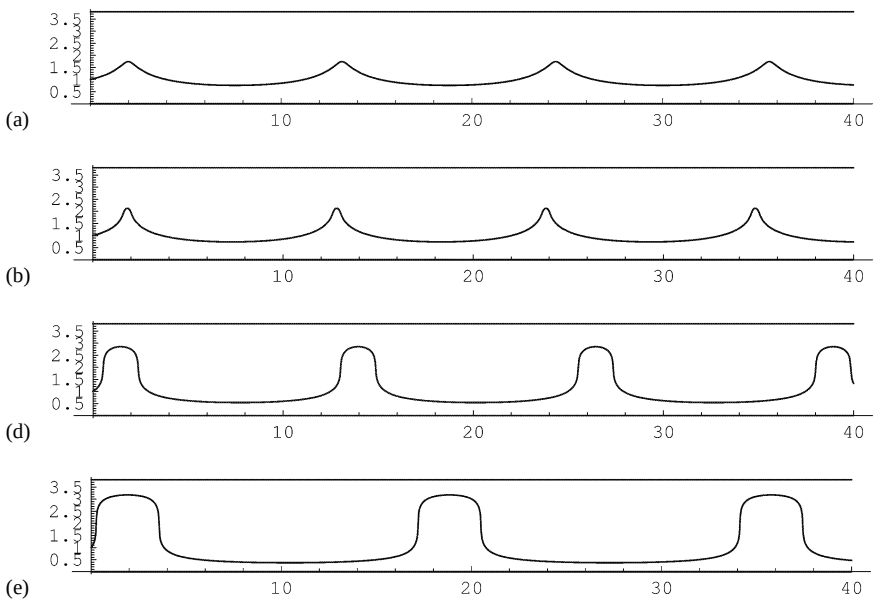


Fig. 8. Nonlinear waves of family B for the same values of the model parameters as in Fig. 4, except for a slightly higher phase speed ($M = 2.1$ instead of $M = 2$), which corresponds to a longer wavelength. The amplitude of the wave on panel (a) is deliberately chosen close to that of Fig. 4(c). The response of the wave to the increase of amplitude, panels (b)–(e), differs significantly from that on Fig. 4. In particular, there is no cusp formation anymore.

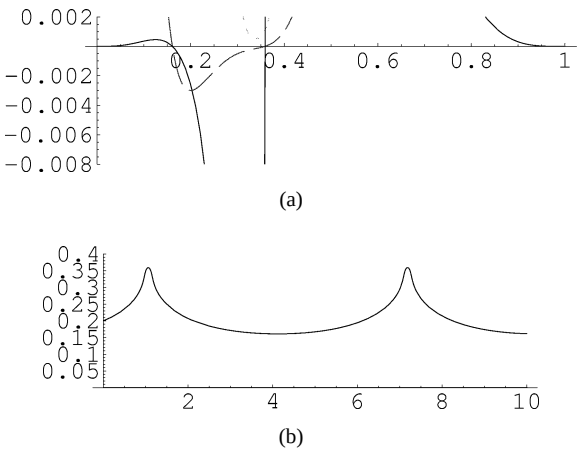


Fig. 9. Same as in Fig. 3, but for a wave of family B. The values of the parameters defining the system $(\gamma, r)$ are the same. The displayed wave has a little higher phase velocity $M = 1.44$; the denominator no longer vanishes, and hence there is no critical amplitude anymore. For the wave shown, $\mathcal{A} = 0.03$.

by increasing the phase speed, i.e., the value of $M$, cf. Fig. 9 and Fig. 3. Similarly, Fig. 8 should be compared with Fig. 4.

Analogously, the family B waves can be obtained for the same parameter values as those used in Fig. 6, by increasing $M$.

## 4. Discussion

We have demonstrated that waves of finite amplitude may propagate at the interface in a two-layer rotating shallow water model. In the limit of small amplitudes they correspond to the classical internal inertia–gravity waves and, therefore, are the finite-amplitude counterparts of these latter. Although the waves are plane-parallel, they are not strictly one-dimensional as they are accompanied by a system of alternating currents in the cross-propagation direction. The two-layer RSW models long-wave perturbations of the sharp density gradient regions in the continuously stratified fluid. So it would be interesting to look for manifestations of these waves in the oceanic thermocline.

The question of stability of the nonlinear wave solutions remains open. It is notoriously difficult

to study stability of the periodic solutions analytically, especially if their analytic expression is unknown. However, preliminary direct numerical simulations show that the waves in question are surprisingly robust in the one-layer RSW. In the two-layer RSW the characteristic shear instabilities come into play. For example, we expect limitations due to the Kelvin–Helmholtz instability to appear in the kink-like waves of the B family: as can be seen from (15), the transverse velocity shear diverges as the interface comes close to the upper and lower boundaries.

## References

[1] A.E. Gill, Atmosphere–Ocean Dynamics, Academic Press, New York, 1982.
[2] R.H.J. Grimshaw, L.A. Ostrovsky, V.I. Shrira, Yu.A. Stepanyants, Surveys Geophys. 19 (1998) 289.
[3] A.C. Kuo, L.M. Polvani, J. Phys. Oceanogr. 27 (1997) 1614.
[4] J. Pedlosky, Geophysical Fluid Dynamics, 2nd Edition, Springer-Verlag, 1987.
[5] V.I. Shrira, Izv. Atmos. Ocean. Phys. 17 (l) (1981) 55.
[6] V.I. Shrira, Izv. Atmos. Ocean. Phys. 22 (4) (1986) 298.
[7] V. Zeitlin, S.B. Medvedev, R. Plougonven, J. Fluid Mech. 481 (2003) 269.